Electronic Supplementary Information

Rational Impurity Doping for enhanced Hole Mobility in Silicon Quantum Dots for Light-Emitting Diodes

Hiroyuki Yamada[*1], Tadaaki Nagao[1] and Naoto Shirahata[*1,2]

[1]International Center for Materials Nanoarchitectonics (MANA), National Institute for Materials Science (NIMS), 1-1 Namiki, Tsukuba, 305-0044, Japan.

[2]Graduate School of Chemical Sciences and Engineering, Hokkaido University, Sapporo 060-0814, Japan.

Experimental Section

Materials

Triethoxysilane (TES) was purchased from Tokyo Chemical Industry Co., Ltd., and used as received. AI 4083 PEDOT:PSS was purchased from Ossila and used with 0.45 μm PTFE filter. Colloidal ink of zinc oxide (ZnO), 10-undecenoic acid, hydrochloric acid (HCl) and molybdenum (IV) oxide (MoO_3, 99.97% trace metal basis), 4,4',4''-Tri(9-carbazoyl)triphenylamine (TCTA, 97%) and TFB were purchased from Sigma-Aldrich and used as received. Electronic-grade hydrofluoric acid (HF, 48% aqueous solution) was purchased from Kanto Chemical Co., Inc. Ethanol (99.5) and boric acid were purchased from Wako Chemical. Milli-Q water (resistivity = 18.2 MΩ·cm) was obtained by Sartorius water purification system (arium 611 UV).

Preparation of Colloidal ink of Boron-doped (p-type) and Undoped SiQDs

The synthesis of p-type SiQDs with a diamond cubic lattice structure began with the preparation of amorphous hydrogen silsesquioxane (HSQ) containing a boron source. Specifically, a 10 mL of TES was placed in a two-neck flask, which was then kept in an ice bath and stirred in an Ar atmosphere. Next, a 20 mL of hydrochloric acid solution adjusted to pH 3 containing 5 mol% boric acid was added dropwise at a constant rate of 1.92 mL/min to hydrolyze the TES molecules. In the case of undoped SiQDs, the same procedure was followed without the addition of boric acid. The resulting white solution was filtered under reduced pressure to obtain white powder (i.e., HSQ). The powder was filtered and washed with milli-Q water until pH 7, then dried overnight under vacuum. The dried powder was transferred to a quartz crucible, placed in a vacuum furnace, and thermally disproportionated at 1100 °C for 2 hrs in 5%-H_2/95%-Ar to obtain a dark brown powder (i.e., SiO_x containing SiQDs). The powder (300 mg) was then ground in an agate mortar using a pestle. The SiO_x was removed by stirring for 90 min in an etchant consisting of 8 mL ethanol and 16 mL 48% HF solution. The HF treatment released hydrogen-capped SiQDs, which were collected by centrifugation at 15,000 rpm for 5 min at 10 °C. To give a colloidal stability, the hydrogen-capped SiQDs were subjected to the thermal hydrosilylation of 10-undecenoic acid; the temperature

was fixed at 180 °C and held for 3 hrs because 10-undecenoic acid monolayers have a higher molecular packing density when heated above 175 °C (see Fig. 1a).[1] The product was centrifuged in a mixture of 1 mL ethanol and 30 mL hexane to remove unreacted 10-undecenoic acid, and redispersed in ethanol at a concentration of 5 mg/mL.

Device Fabrication

Si-QLEDs were fabricated on a glass substrate coated with a thin ITO film pattern with size 2 mm × 20 mm, 130 nm thickness (Resistivity of 10-14 Ω/sq). First, the substrate was cleaned by ultrasonic agitation with acetone, isopropanol and ethanol respectively. After drying, the substrate was exposed to VUV light (λ = 172 nm and 10 mW/cm^2, Ushio Corp.) for 30 min under a pressure of 10^3 Pa and N_2 flow and the water contact angle changed from about 40° to less than 5° on the ITO surface, indicating super hydrophilicity.[2] This superhydrophilicity is ideal for spin-coating an isopropanol suspension of colloidal ZnO, as it allows the suspension to closely wet and adhere to the hydrophilic substrate during film formation. As a result, the intimate contact between the ITO and ZnO layers facilitates more efficient charge transfer across the ITO-ZnO interface. Second, the colloidal ink of ZnO was spin-coated with a rotation speed of 2,000 rpm for 60 s in Ar-filled glovebox, and annealed at 120 °C, followed by spin-coating of the ethanol solution of QD with a speed of 1,000 rpm for 60 s. Third, the sample was transferred into a vacuum chamber and vacuumed to 2×10^{-5} Pa. A HTL of TCTA and a HIL of MoO_3 were thermally evaporated on the QD layer in that order. Finally, the Ag top electrode was deposited with a stainless mask (10 mm × 2 mm) over the film.

Characterization

X-ray powder diffraction (MiniFlex600, Rigaku, Japan) was employed to detect the crystalline phase. ICP-OES analysis (Agilent 5800, Agilent Technologies, Inc., USA) was employed to determine the boron content in hydrogen-capped SiQDs. An UV-VIS spectrum was measured by a UV-VIS spectrophotometer (V-650, JASCO, Japan). Fourier transform infrared spectroscopy (FTIR) was performed by iS50R (Thermo Fisher Scientific, USA) coupled to mercury-cadmium-telluride detector.

For the transmittance analysis, the QD sample was dropped on a Si wafer. Photoluminescence (PL) spectrum was measured using a NanoLog spectrofluorometer by Horiba Jovin Yvon. To minimize interference from scattered excitation light, a 495 nm cut-off filter was placed in front of the monochromator-PMT assembly. Absolute PLQY was measured at room temperature using the C9920-02 QY system from Hamamatsu Photonics Co., Ltd., an integrating sphere as the sample chamber, and a multichannel analyzer for signal detection. Ultraviolet photoelectron spectroscopy (UPS, SigmaProbe, Thermo Fisher Scientific, Inc., USA) was used to determine the Fermi energy and the valence band maximum (VBM) energy levels. Device characterization was performed using a calibrated silicon photodetector (S1336-8BQ, Hamamatsu Photonics Co., Ltd., Japan) in conjunction with a Keithley 2635B source meter.

Observation and Analysis of Microstructures

Cross-sectional scanning electron microscopy (SEM) was operated at 1 kV under a 54° tilt angle using a ZEISS Auriga Laser (Carl Zeiss, Germany) integrated with a focused ion beam (FIB) equipped with a Ga^+ ion source. The FIB process involved the deposition of a carbon protective layer (with carbon gas) followed by the formation of a gap to expose the cross-sectional observation surface.

Preparation of Sample solutions for ICP-OES Measurements

Approximately 5 mg of hydrogen-capped boron(B)-doped SiQDs or undoped SiQDs was accurately weighed and transferred into a 100 mL perfluoroalkoxy alkane (PFA) beaker. Next, 10 mL of a nitric acid (1+1) solution and 1 mL of HF were added, followed by thermal decomposition under controlled heating. After cooling to room temperature, the resulting solution was transferred to a 100 mL polypropylene (PP) volumetric flask. Manganese (Mn) was added as an internal standard at a concentration of 1 mg. The solution was then diluted to the mark with Milli-Q water prior to ICP-OES measurement.

Calculation of EQE and Optical Power Density

EQE and optical power density were determined under the assumption that the EL follows a Lambertian emission profile-an approximation commonly adopted

for bottom-emitting QLED architectures that lack strong microcavity effects, where the angular distribution of EL intensity typically exhibits Lambertian-like behavior.[3] EQE is defined as a ratio of the number of emitted photons to the number of injected electrons per unit time, expressed as $I_d(V)/|e|$, where $I_d(V)$ is the current flowing through the device at an applied voltage V, and e is the elementary charge of an electron. The EQE was calculated using the following equation:[4]

$$\mathrm{EQE}\ (\%) = \frac{N_p(V) \times |e| \times g}{I_d(V)} \times 100 \qquad (1)$$

Here, $N_p(V)$ represents the number of photons detected by the photodiode, and g, the geometry factor, accounts for the ratio of the luminous flux emitted by the LED to the flux measured by the photodiode. The geometry factor g is given by the equation:

$$g = \frac{a^2 + L^2}{a^2} \qquad (2)$$

Here, a represents a radius of the aperture of the photodiode, and L denotes the distance between the light-emitting surface and the photodiode. The calculated g value was 2.49. Details of the calculation are provided in Fig. S1, ESI†. The number of photons $N_p(V)$, derived from the EL spectrum. The photodiode current I_p^m, is given by the following equation:

$$N_p(V) = \int_{\lambda_i}^{\lambda_f} EL(\lambda) \times \frac{I_p^m}{I_p'(\lambda)} d\lambda \qquad (3)$$

Here, $I_p'(\lambda)$ is expressed in terms of Planck's constant h, the speed of light in vacuum c, the EL emission wavelength λ, and the photodiode responsivity $R(\lambda)$. It is calculated using the following equation:

$$I_p'(\lambda) = \int_{\lambda_i}^{\lambda_f} EL(\lambda) \times \frac{hc}{\lambda} \times R(\lambda)\, d\lambda \qquad (4)$$

By calculating $N_p(V)$ for all applied voltages and substituting it into Eq.1, the voltage- or current density-dependent EQE characteristics can be obtained. The optical power density was determined as follows: the emitted power $P(V)$ is calculated using the equation:

$$P(V) = \int_{\lambda_i}^{\lambda_f} EL(\lambda) \times \frac{I_p^m}{I_p'(\lambda)} \times \frac{hc}{\lambda} d\lambda \qquad (5)$$

The optical power density is then given by:

$$\text{Optical power density (W/cm}^2) = \frac{P(V)}{A} \qquad (6)$$

where A represents the area of the light-emitting surface.

Electron only device (EOD) fabrication

First, ITO-coated substrates were cleaned by UV ozone cleaning at 30 min under a pressure of 10^3 Pa and N_2 flow. Next, the colloidal ink of ZnO was spin-coated with a rotation speed of 2,000 rpm for 60 s. After drying the film at 120 °C under atmosphere, the active layer of the SiQDs was spin-coated with a concentration of 5 mg/mL in ethanol with a speed of 1,000 rpm for 60 s. After drying the film at 120 °C under Ar, the colloidal ink of ZnO was spin-coated with a rotation speed of 2,000 rpm for 60 s. Finally, the Ag top electrode was deposited with a stainless mask over the film with a vacuum level of 2×10^{-5} Pa.

Hole only device (HOD) fabrication

Initially, PEDOT:PSS was spin-coated on the ITO-coated substrate with a rotation speed of 5,000 rpm and drying the film at 140 °C under atmosphere. Next, TFB was spin-coated with a concentration of 1.8 wt% in toluene with a speed of 2,000 rpm for 60 s. After drying the film at 120 °C under Ar, SiQDs was spin-coated with a concentration of 5 mg/mL in ethanol with a speed of 1,000 rpm for 60 s. Then, a hole transportation layer (HTL) of TCTA and a hole injection layer (HIL) of MoO_3 were thermally evaporated with a vacuum level of 2×10^{-5} Pa. Finally, the Ag top electrode was deposited with a stainless mask over the film with a vacuum level of 2×10^{-5} Pa.

References

1. N. Shirahata, *Sci. Rep.*, 2022, **12**, 17211.
2. N. Shirahata and A. Hozumi, *Chem. Mater.*, 2005, **17**, 20.
3. N. C. Greenham, R. H. Friend and D. D. C. Bradley, Advanced Materials, 1994, **6**, 491-494; W. Jin, Y. Deng, B. Guo, Y. Lian, B. Zhao, D. Di, X. Sun, K. Wang, S. Chen, Y. Yang, W. Cao, S. Chen, W. Ji, X. Yang, Y. Gao, S. Wang, H. Shen, J. Zhao, L. Qian, F. Li and Y. Jin, *npj Flexible Electronics*, 2022, **6**, 35; X. Dai, Z. Zhang, Y. Jin, Y. Niu, H. Cao, X. Liang, L. Chen, J. Wang and X. Peng, *Nature*, 2014, **515**, 96-99; Shen, H. et al. H. Shen, Q. Gao, Y. Zhang, Y. Lin, Q. Lin, Z. Li, L. Chen, Z. Zeng, X. Li, Y. Jia, S. Wang, Z. Du, L. S. Li and Z. Zhang, *Nat Photonics*, 2019, **13**, 192-197; G. Zaiats, S. Ikeda and P. V. Kamat, *NPG Asia Mater*, 2020, **12**, 57.
4. G. J. S. Supran, *Ph.D. Thesis, Massachusetts Institute of Technology, Cambridge, MA, USA*.

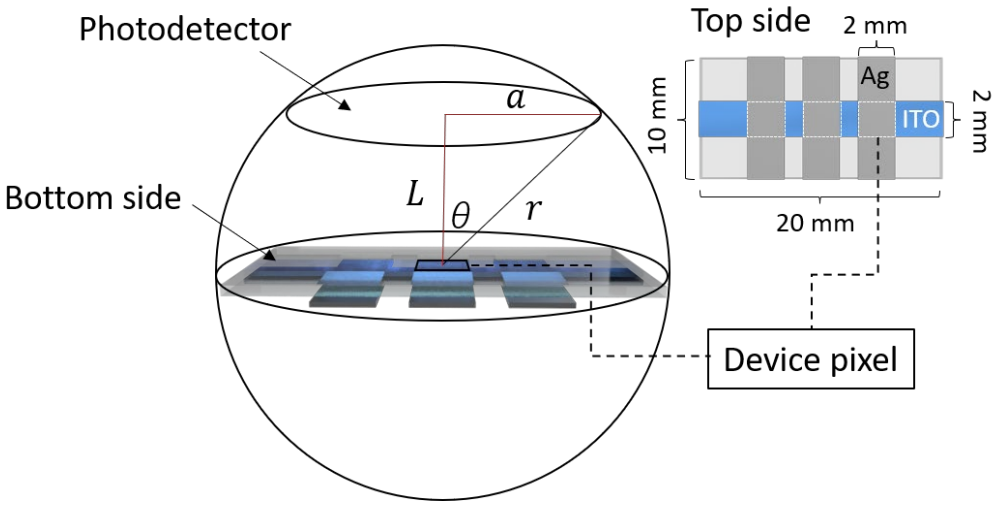

Fig. S1 Schematic diagram of the photocurrent measurement setup. The emissive device is electrically biased, and its emitted light is collected by a calibrated photodetector of radius $\boldsymbol{a}$, giving an active area $\boldsymbol{S = \pi a^2}$. The detector is positioned at a distance $\boldsymbol{L}$ from the emission surface, and $\boldsymbol{\theta}$ is defined as the angle between $\boldsymbol{L}$ and $\boldsymbol{r}$.

As shown in Fig. S1**,** a photodetector of active area S is positioned at a distance L from the emission surface. Let us model the detector as subtending a portion of a hemisphere of radius

$$r = \sqrt{a^2 + L^2}$$

where a is the detector's active area radius. The corresponding solid angle Ω is

$$\Omega = \pi sin^2\theta = \frac{S}{r^2} = \pi\left(\frac{a}{\sqrt{a^2 + L^2}}\right)^2 = \frac{a^2\pi}{a^2 + L^2}$$

If $P_{measure}$ is the photocurrent collected by this detector, then the photocurrent per steradian, P_0, satisfies the ratio,

$$1 : P_0 = \frac{a^2\pi}{a^2 + L^2} : P_{measure}$$

$$\therefore P_0 = \left(\frac{a^2 + L^2}{a^2\pi}\right) P_{measure}$$

Because the total solid angle of a hemisphere is π sr, the total photocurrent P_{total} emitted into the hemisphere is

$$P_{total} = \pi P_0 = \pi\left(\frac{a^2 + L^2}{a^2\pi}\right) P_{measure} = \left(\frac{a^2 + L^2}{a^2}\right) P_{measure}$$

Therefore, the geometric factor,

$$g = \frac{P_{total}}{P_{measure}} = \frac{a^2 + L^2}{a^2}$$

Substituting $a = 3.2723\,mm$ and $L = 4\,mm$ yields

$$g = 1 + \frac{L^2}{a^2} = 1 + \frac{4^2}{3.2723^2} \approx 2.49$$

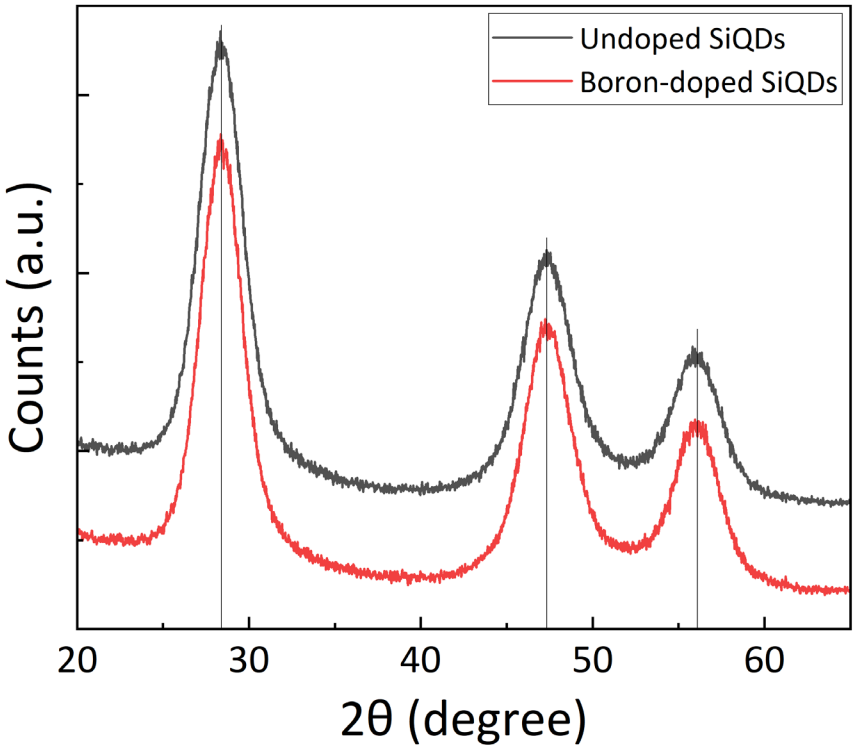

Fig. S2 XRD patterns of hydrogen-capped SiQDs with and without boron doping. The hydrogen termination effectively suppresses surface oxidation, resulting in the absence of detectable SiO_2 peaks around 20°.

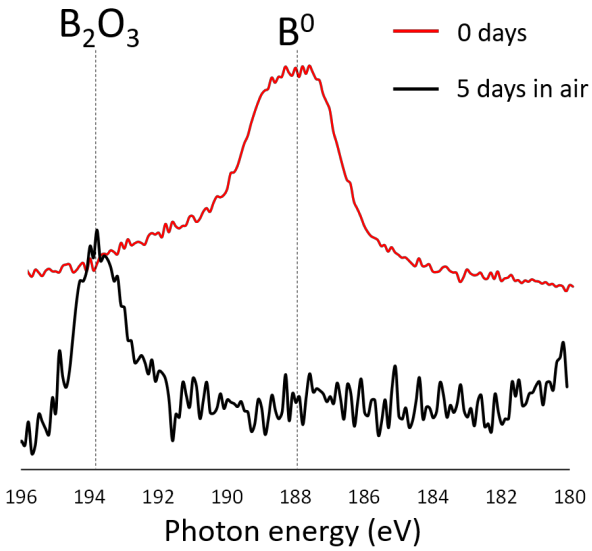

Fig. S3 XPS B1s spectra of hydrogen-capped SiQDs synthesized with a nominal 5 mol% boron content, measured immediately after preparation (red line) and after 5 days of exposure to ambient atmosphere (black line).

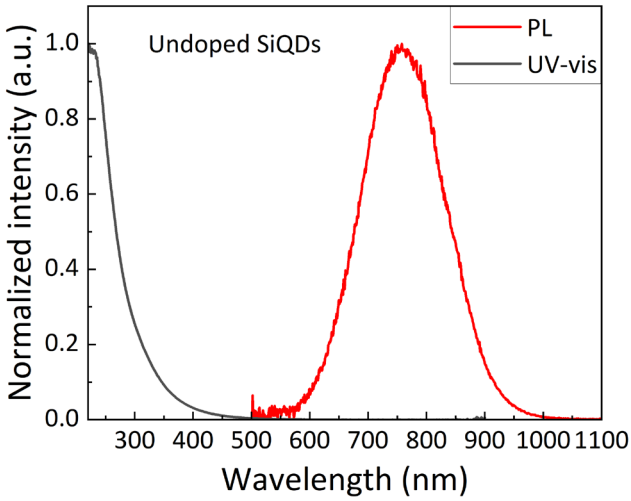

Fig. S4 UV-VIS and PL spectra of the undoped SiQDs terminated with undecanoic acid monolayers.

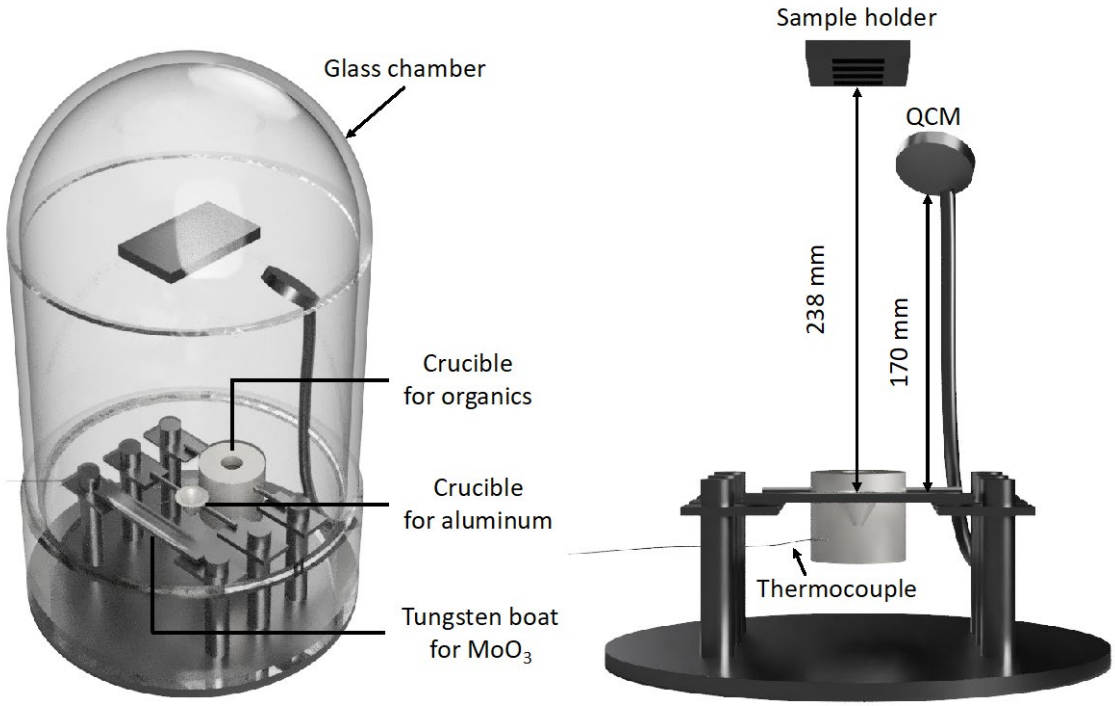

Fig. S5 The schematic illustration of thermal evaporation machine and a detailed illustration of the setup.

In this study, we found that the organic material crucible requires a system capable of uniformly heating the contents to control the evaporation rate and ensure the formation of high-quality films. Accordingly, we used a CH-14 crucible (Nilaco Co., Ltd., Japan) for the evaporation of organic compounds. To prevent contamination of the vacuum chamber base, an alumina-coated tungsten basket (B-3, Nilaco Co., Ltd., Japan) was used as the crucible for electrode materials (e.g., aluminum, silver). Additionally, a tungsten boat (SF-110, Nilaco Co., Ltd., Japan) was employed for MoO_3 evaporation.

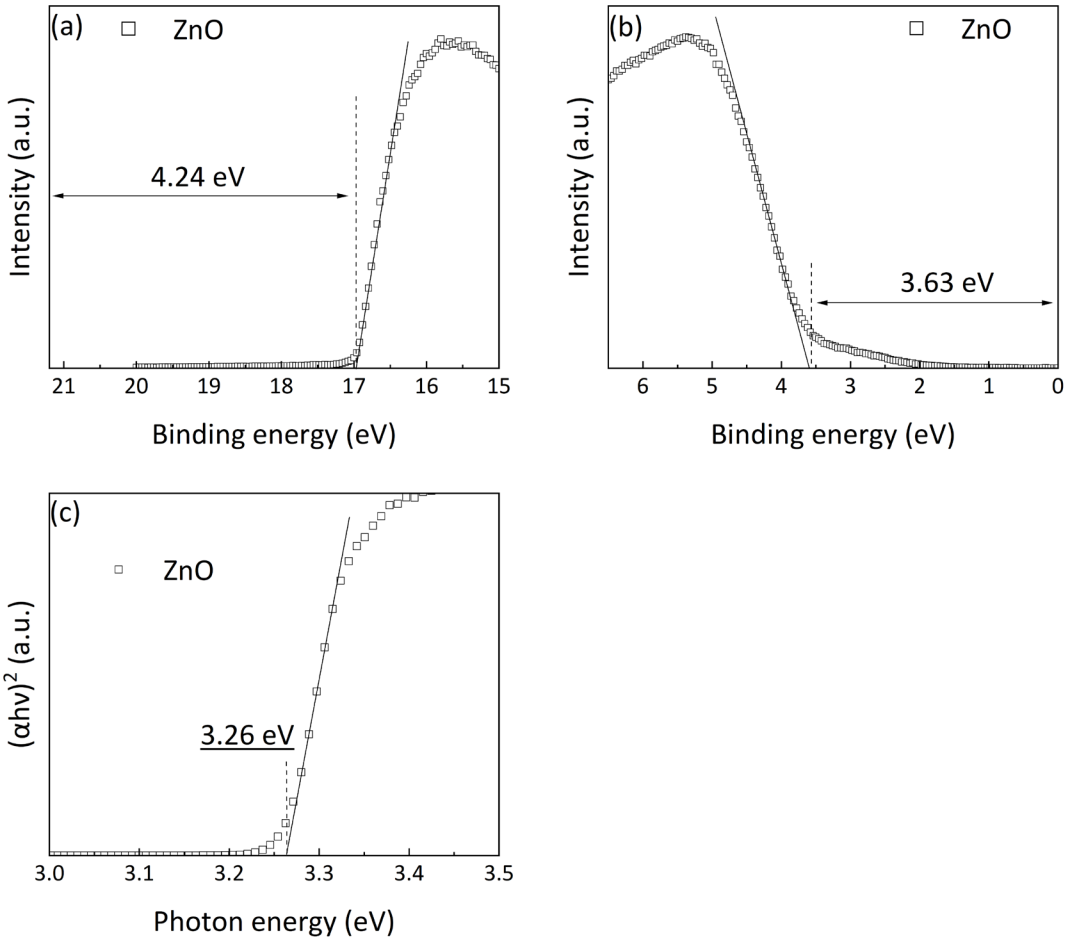

Fig. S6 Ultraviolet photoelectron spectroscopic (UPS) spectra of (a) the secondary-electron cutoff and (b) valence-band edge regions of ZnO thin film are displayed. (c) The $(\boldsymbol{\alpha h\nu})^2$-$\boldsymbol{h\nu}$ plot obtained from the UV-VIS spectrum.

The work function was determined from the energy difference between the secondary electron cut-off and the excitation photon energy ($h\nu$ = 21.22 eV). Based on this, the valence band maximum (VBM) was estimated to be 7.87 eV. Given the optical bandgap of the sample (E_g = 3.26 eV), the conduction band minimum (CBM) was subsequently calculated to be 4.61 eV.

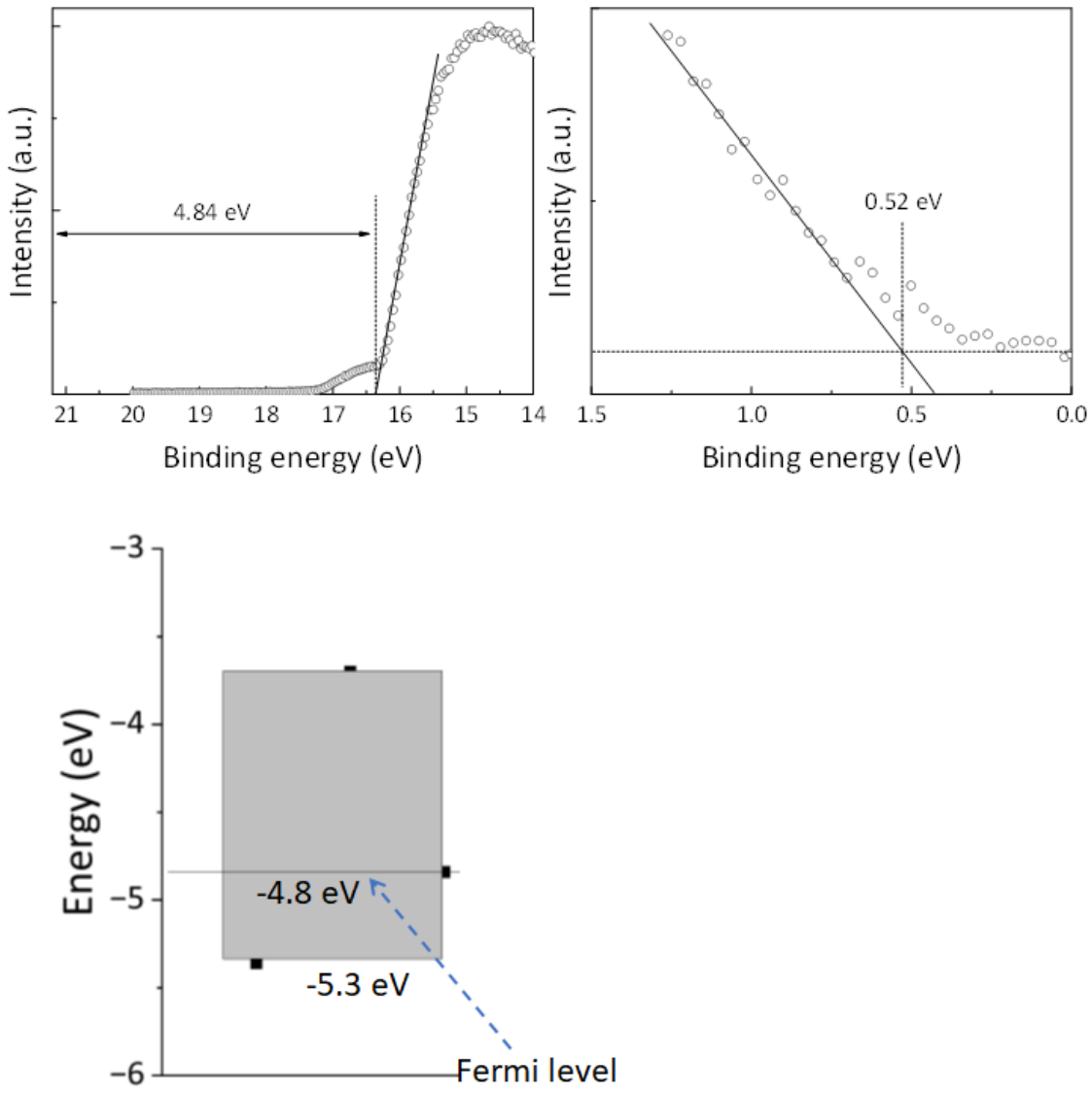

Fig. S7 UPS spectra of the boron-doped SiQDs terminated with undecanoic acid monolayers. As the work function is calculated by the difference in energy between the secondary electron cutoff and the excitation photon energy ($h\nu$ = 21.22 eV), the VBM value is estimated to be 5.36 eV. Fermi energy level positions at 4.84 eV, being close to VBM for p-type conductivity (modified from Fig. 1(i) and 1(j) in Ref. 16).

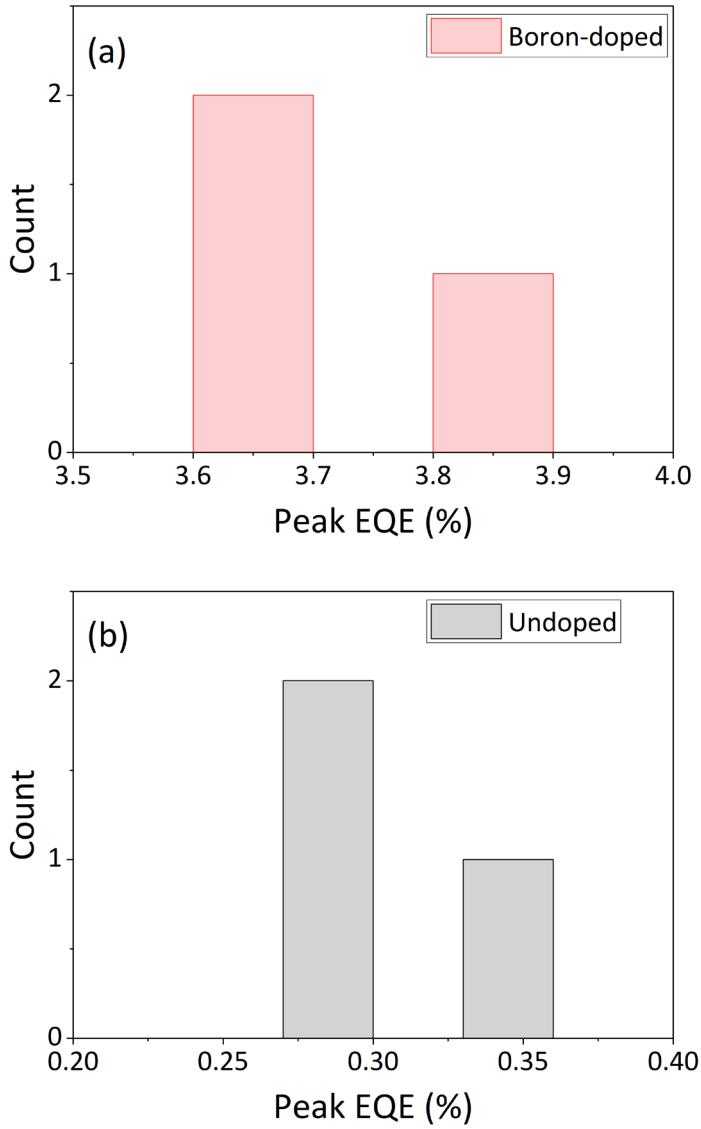

Fig. S8 Histograms of peak EQEs for three Si-QLED devices: (a) boron-doped and (b) undoped SiQDs were used as emission layers of the devices. The estimated EQEs of the boron-doped Si-QLEDs were 3.60%, 3.65%, and 3.85%, while those of the undoped Si-QLEDs were 0.27%, 0.28%, and 0.35%, respectively.

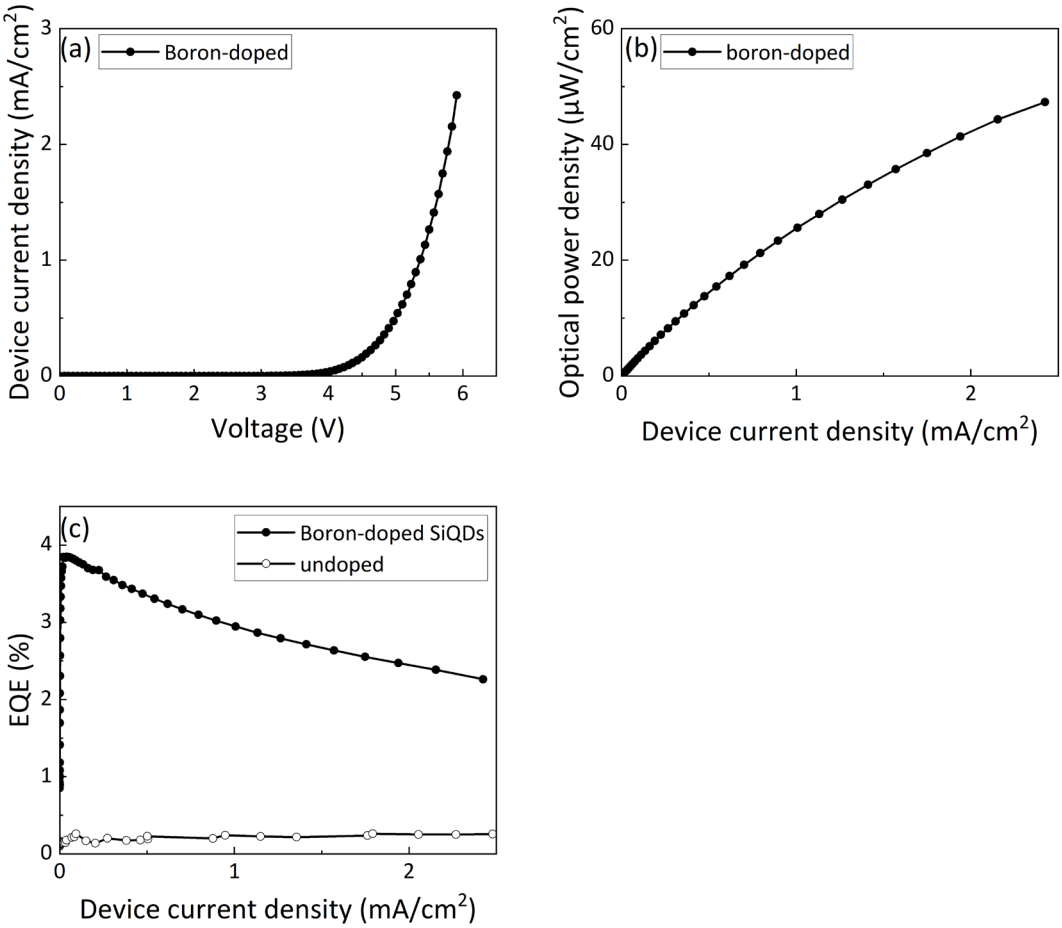

Fig. S9 Device performances of the boron-doped Si-QLED that exhibited an EQE of up to 3.85% (see Fig. S8): (a) *I*–*V* characteristics, (b) optical power density and (c) EQE as a function of device current density plotted with the undoped device.

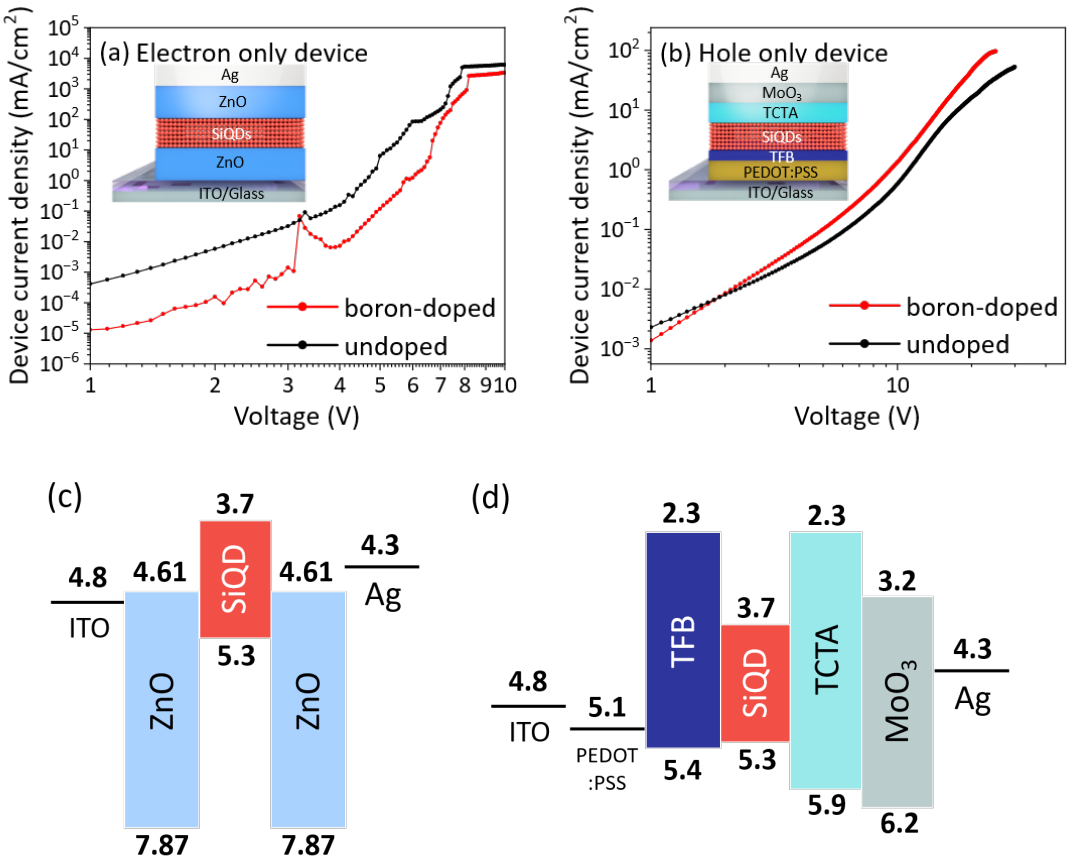

Fig. S10 *J-V* characteristics of electron only device (EOD) with device structure of ITO/ZnO/SiQD/ZnO/Ag and (b) hole only device (HOD) with device structure of ITO/PEDOT:PSS/TFB/SiQD/TCTA/MoO_3/Ag. (c,d) Flat energy band diagrams corresponding to the EOD and HOD, respectively.